

Supplementary Material

Axisymmetric gravity currents within porous media: first order solution and experimental validationSandro Longo¹, Vittorio Di Federico²

The present Supplementary material, made available online, presents a more extensive comparison of first-order results with laboratory experiments, illustrating results for: i) the current profile in tests #17 and #18 of Longo et al. (2013); ii) the current profile in tests #1, #2 and #5 of Lyle et al. (2005); iii) the current radius in test #16 of Longo et al. (2013).

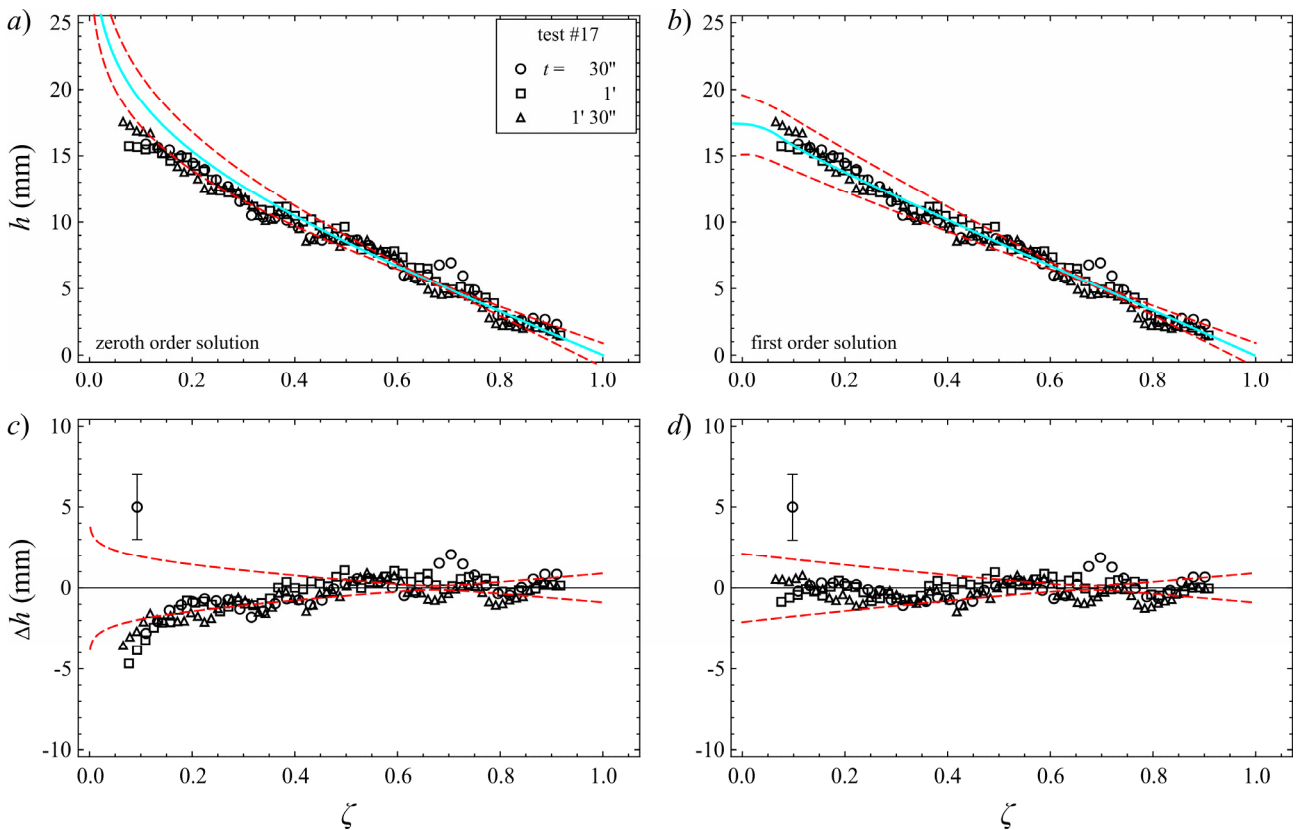
1. The current profile in the experiments of Longo et al. (2013)

Figure S1. *a)* The height of the gravity current as a function of radial coordinate, zeroth order solution. *b)* First order solution. *c)* Residuals for the zeroth order solution and *d)* for the first order solution. The dashed lines are the 95% confidence limits, the error bar indicates the uncertainty at 95% level of confidence. Results for test #17, $\mu = 0.012 \pm 3.5\%$ Pa-s, $\Delta\rho = 1145 \pm 1\%$ kg/m³, $Q_d = 4.0 \pm 0.5\%$ ml/s, $\alpha = 1.0$, $d = 3.0 \pm 5\%$ mm, $\phi = 0.38 \pm 1\%$.

Figure S1 is analogous to Figure 5 but for test #17; results are qualitatively similar, except that the fitting is better and confidence intervals are narrower. When the coefficient of variation of the

current height is depicted as a function of ζ , results are again qualitatively similar to those of test #16 (see Figure 6 in the main manuscript), but with a lower CV.

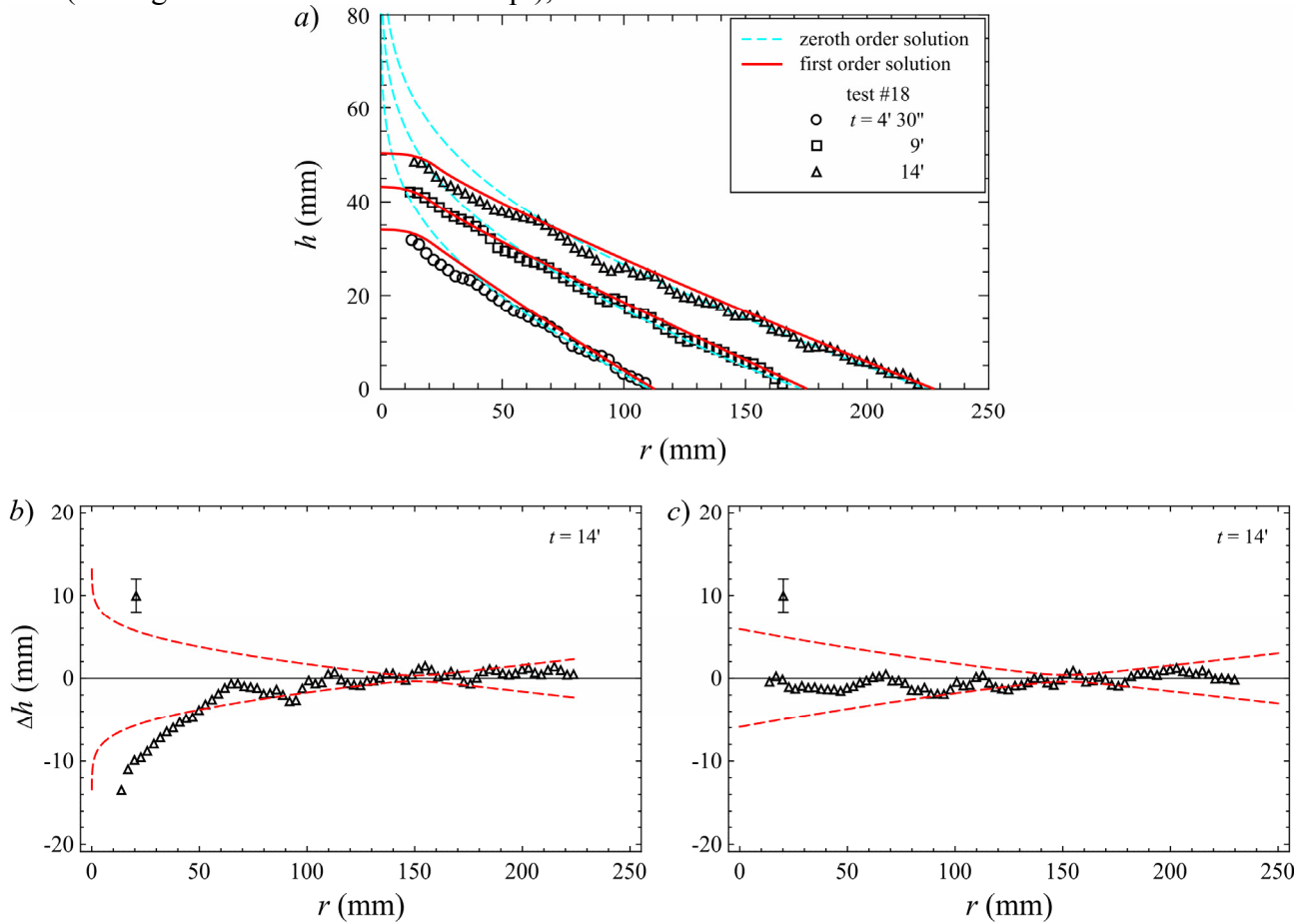


Figure S2. *a)* The height of the gravity current as a function of radial coordinate. Dashed line: zeroth order solution. Bold line: first order solution. Symbols: *b)* Residuals for the zeroth order solution at $t = 14'$ and *c)* for the first order solution for the current profile at the same time. The dashed lines are the 95% confidence limits and the error bar indicates the uncertainty at 95% level of confidence. Results for test #18, $\mu = 0.26 \pm 3.5\%$ Pa·s, $\Delta\rho = 1241 \pm 1\%$ kg/m³, $Q_d = (0.06 \pm 0.5\%) t^{1/2}$ ml/s, $\alpha = 1.5$, $d = 3.0 \pm 5\%$ mm, $\phi = 0.38 \pm 1\%$.

Figure S2a shows the comparison between the experimental height data and the theoretical models for test #18 with $\alpha = 1.5$ at three different times. Figure S2bc show the residuals for the zeroth order and first order solution. It is noted that the first order solution provides a more than satisfactory fit to experimental data at all times as shown also by the low value of residuals.

2. The current profile in the experiments of Lyle et al. (2005)

Figure S3 shows the data from experiments 1, 2 and 5 as a function of the reduced similarity variable. For all tests the first order solution yields a much better agreement with the experimental data near the origin (i.e. $\zeta < 0.2$) than the zeroth order one.

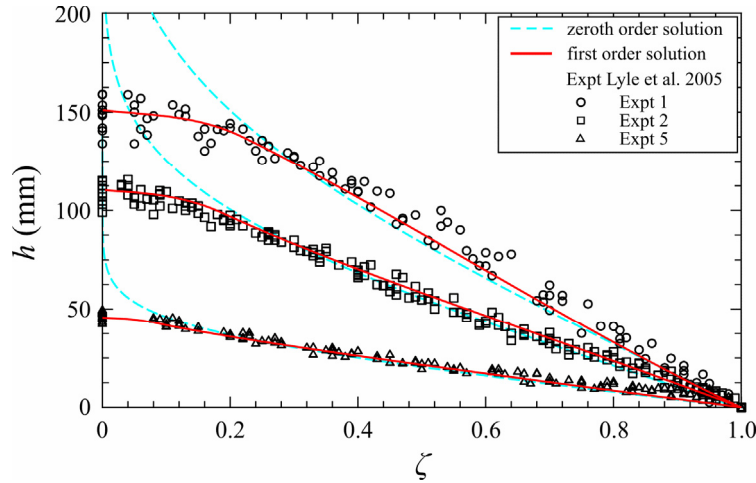


Figure S3. The height of the gravity current as a function of the scaled variable ζ . Symbols: experiments from Lyle et al. (2005). Dashed line: zeroth order solution. Bold line: first order solution.

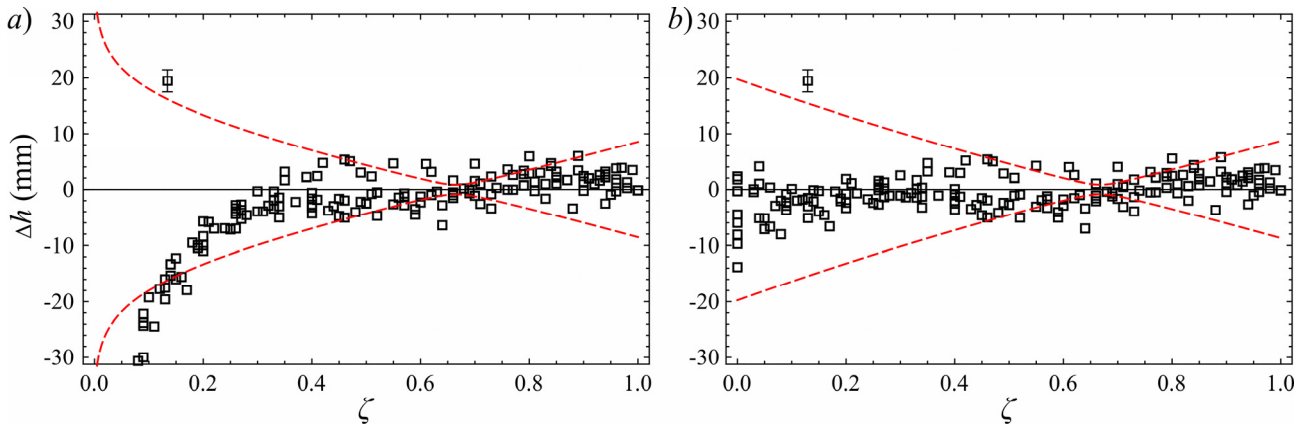


Figure S4. a) The residuals with respect to the zero order solution and b) to the first order solution. The dashed lines indicate the 95% confidence limits and the error bar indicates the uncertainty at 95% level of confidence. Expt 2 from Lyle et al., 2005, $\mu = 1.2 \cdot 10^{-3} \pm 3.5\%$ Pa·s, $\Delta\rho = 20.4 \pm 0.3$ kg/m³, $Q_d = 34.4 \pm 0.2$ ml/s, $\alpha = 1.0$, $d = 3.0$ (-0.15,+0.30) mm, $\phi = 0.37 \pm 1\%$.

Figure S4ab, depicting the residuals respectively for zeroth order and first order solution for Expt. 2, demonstrate again the narrowing of confidence limits associated with the first order correction. Performing an analogous analysis of the remaining experiments by Lyle et al. (2005) yields residuals and associated confidence limits that are qualitatively similar to those illustrated for experiment 2 and those derived in the experiments by Longo et al. (2013). To provide a comprehensive re-examination of Lyle et al.'s experiments, Table S1 lists the maximum height measured in the origin and that estimated with the first order solution. The uncertainties refer to 95% level of confidence (roughly two standard deviations).

Table S1. Measured maximum height at the origin for experiments 1-6 by Lyle et al. (2005) and height in the origin estimated with first order solution. h_{\max} is the experimental value, h_{est} is the estimated value with the first order solution. The uncertainties refer to 95% level of confidence.

Expt	1	2	3	4	5	6
h_{\max} (cm) at $r=0$	13.4±0.2	11.7±0.2	8.9±0.2	7.3±0.2	5.0±0.2	13.4±0.2
h_{est} (cm) at $r=0$	15.1±3.1	11.5±2.1	8.7±1.3	6.5±1.1	4.5±0.7	12.7±2.0

The estimated and the measured height of the current at the origin are shown to be statistically equal. Indeed observing all the documented height profiles, their almost linear shape fits the first order solution, confirming the functional form suggested by Lyle et al. (2005) who indicate the expression $h/(Q_d/g')^{1/2} = 9.2(1 - \zeta)$ to interpret their experimental results for $\zeta > 0.2$ (g' is the reduced gravity, the left hand term and the coefficient are in $s^{-1/2}$).

3. Radius of the intruding current in the experiments of Longo et al. (2013)

A second important output of the experiments by Longo et al. (2013) is represented by the front end of the current at different times. The experimental radius is evaluated by analysing the photos from the bottom, detecting the boundary of the intruding current and averaging over a 90° arc. For the zeroth order solution, the theoretical prediction of the spreading rate of the current is a monomial expression including the model parameters and proportional to $t^{(\alpha+1)/4}$ (see Lyle et al., 2005). For the first order solution the spreading rate is slightly larger at early times and later, for large values of r_N , tends to behave as for the zeroth order solution case. By applying the same technique already adopted for the height of the current, it is possible to evaluate the contribution due to the uncertainty in the parameters. Each contribution is proportional to $\sim t^{(\alpha+1)/4}$ hence the relative contribution, and the coefficient of variation, are constant over time.

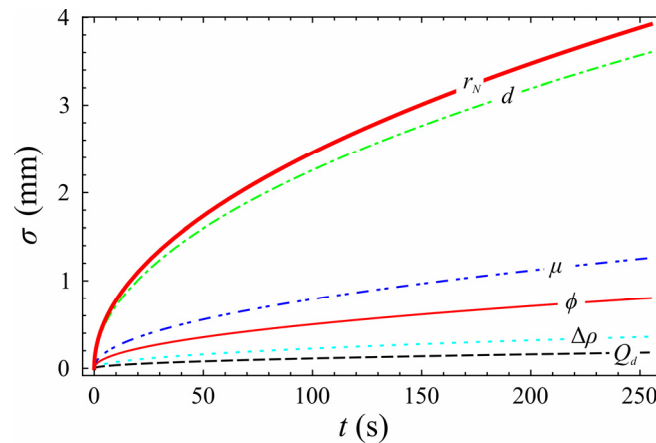


Figure S5. Contributions to the standard deviation of the radius of the intruding current for test #16, $\mu = 0.58 \pm 3.5\%$ Pa·s, $\Delta\rho = 1250 \pm 1\%$ kg/m³, $Q_d = 4.0 \pm 0.5\%$ ml/s, $\alpha = 1.0$, $d = 3.0 \pm 5\%$ mm, $\phi = 0.38 \pm 1\%$.

Figure S5 illustrates the contributions of the uncertainty in the parameters to the standard deviation of the radius of propagation; its inspection shows the predominant influence of the beads diameter.

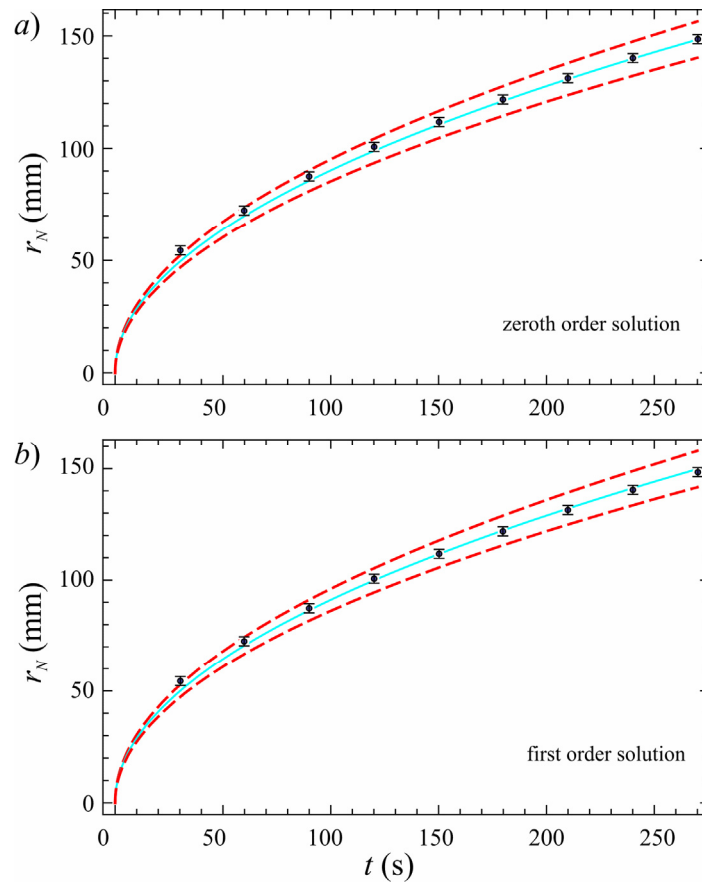


Figure S6. The radius of propagation as function of time for Test #16. a) Zeroth order solution, b) first order solution. The dashed curves and the error bars refer to a 95% level of confidence.

Figure S6ab show the experimental data and the theoretical models in terms of radius of propagation for Test#16; the residuals for the same test are shown in Figure S7ab. It is seen that adoption of either model is immaterial in interpreting experimental results in terms of the radius of propagation.

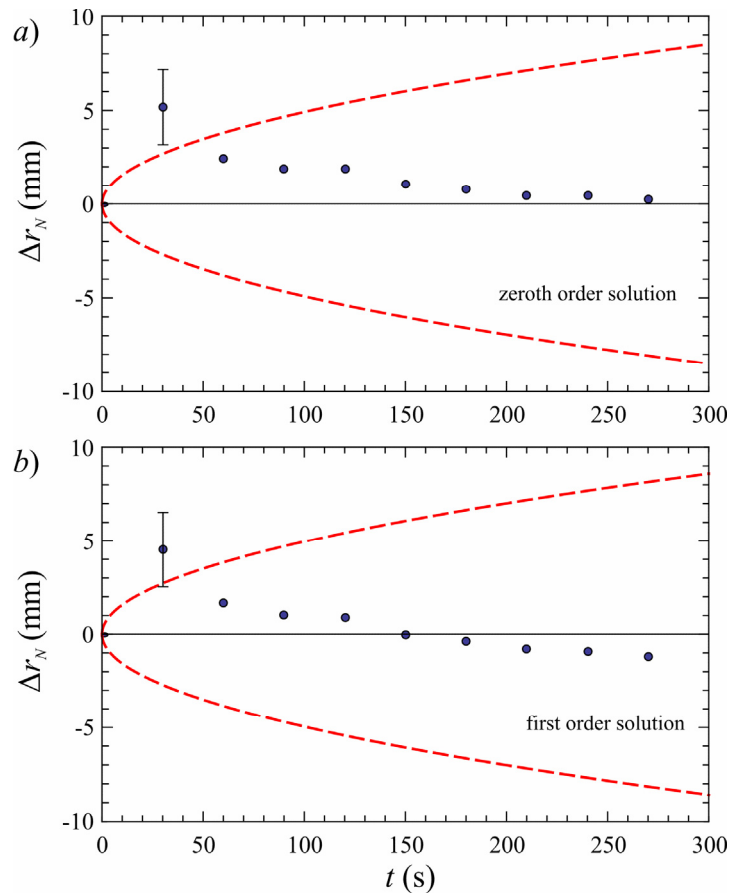


Figure S7. The residuals of the front end position as function of the time with respect to *a*) the zeroth order solution and to *b*) the first order solution. Symbols: difference between the radius of the intruding current from the experiment and from the theoretical model. Dashed lines: the 95% confidence limits of the model. Error bars: the uncertainty in the measurements of the front end position with a 95% level of confidence. Test #16, parameters: $\mu = 0.58 \pm 3.5\%$ Pa·s, $\Delta\rho = 1250 \pm 1\%$ kg/m³, $Q_d = 4.0 \pm 0.5\%$ ml/s, $\alpha = 1.0$, $d = 3.0 \pm 5\%$ mm, $\phi = 0.38 \pm 1\%$. The values of the parameters represent the estimate of the average \pm the standard deviation.

A similar comparison was not carried out for Lyle et al. experiments since the data were not available.

References

- Longo S, Di Federico V, Chiapponi L, Archetti R. Experimental verification of power-law non-Newtonian axisymmetric porous gravity currents. *J Fluid Mech/Rapids* 2013; 731, R2.
- Lyle S, Huppert HE, Hallworth M, Bickle M, Chadwick A. Axisymmetric gravity currents in a porous medium, *J Fluid Mech* 2005; 543: 293-302.